Fuel Processing Technology 156 (2017) 473–484

Contents lists available at ScienceDirect

Fuel Processing Technology

journal homepage: www.elsevier.com/locate/fuproc

Research article

Numerical investigation of microwave-assisted pyrolysis of lignin

Siddharth Gadkari[a], Beatriz Fidalgo[b,*], Sai Gu[a,*]

[a]Department of Chemical and Process Engineering, University of Surrey, Guildford GU2 7XH, United Kingdom
[b]School of Energy, Environmental Technology and Agrifood, Cranfield University, Bedforshire MK43 0AL, United Kingdom

ARTICLE INFO

Article history:
Received 23 August 2016
Received in revised form 4 October 2016
Accepted 6 October 2016
Available online 20 October 2016

Keywords:
Biomass
Lignin
Pyrolysis
Microwave heating
3D Mathematical model

ABSTRACT

A comprehensive three-dimensional mathematical model is developed for studying the microwave-assisted pyrolysis of biomass. Kraft Lignin is considered as biomass feedstock in the model, and a mixture of lignin and char, is used as the sample for pyrolysis. A lumped kinetic model which considers three lumped pyrolysis products (gas, liquid and remaining solid fractions) is coupled with the governing equations for the microwave field, heat transfer, mass transfer, Darcy fluid flow and a transient numerical analysis is performed. The distribution of electric field in the microwave cavity, and the distribution of electric field, temperature, and pyrolysis products within the lignin sample are presented. The lignin sample is predicted to undergo volumetric heating when subjected to microwave heating. Accordingly the reaction zone extends from the center of the biomass sample bed towards the outer surface. Preliminary evaluation of the applicability of the model for assessing the effect of different parameters on the microwave pyrolysis of lignin is also carried out.

1. Introduction

Increasing concerns about the impact of greenhouse gas emissions from the use of fossil fuels coupled with the increasing demand for global energy have stimulated growing interests in renewable energy sources. Biomass is the only renewable energy source of carbon and is therefore called to play a significant role in the transition to a sustainable energy future [1]. Valuable energy can be extracted from biomass fuels via a number of thermochemical and biochemical processes.

Pyrolysis refers to the thermochemical decomposition of a material in the absence of air/oxygen. Pyrolysis can be potentially used for the production of large number of chemical compounds from biomass, which are typically lumped into three main fractions: solid (char), liquid (tar and other condensable organic volatiles) and non-condensable gases [2]. The relative amount of each product fraction depends on number of factors such as feedstock composition, temperature, heating rate and vapour residence time. In other words, biomass pyrolysis process conditions can be modified depending on the final product requirements. Thus, liquid product is maximized by performing the pyrolysis at moderate temperatures with high heating rate and short hot vapour residence time; solid char yield is enhanced at low temperature and low heating rates; and, formation of gaseous products is increased at high temperature, high heating rate and long hot vapour residence time [2]. Research on biomass pyrolysis is gaining increasing importance also as initial stage for many biomass fuel utilization routes. Pyrolysis constitutes the first stage in all thermochemical conversion processes, and has an effect on the fuel reactivity during subsequent gasification and combustion stages.

Small-to-large scale pyrolysis processes have been traditionally heated via external sources such as electric or gas heater, oil bath, furnace or heating mantle in which heat is transferred from the surface to the core of the materials giving rise to a temperature gradient within the heated feedstock material [3–5]. These conventional heating sources require first the heating unit/system to get hot and the heat to be transferred to the biomass particles via conduction, convection or radiation, which inevitably results in a decrease in efficiency.

Compared to conventional sources, microwave heating involves the interaction of the electric field component of the electromagnetic radiation with the charged particles of the heated material, and the subsequent transformation of the microwave energy into thermal energy. Heat is induced due to friction caused by the intermolecular collisions of the charged particles and/or dipoles which attempt to continuously realign in phase with the alternating field of the microwaves [4,6,7]. Contrary to conventional heating, microwave heating mechanism gives rise to selective, fast and volumetric heating, such that the whole material can be heated up almost uniformly [3]. Microwave heating largely depends on the dielectric

* Corresponding authors.
E-mail addresses: b.fidalgofernandez@cranfield.ac.uk (B. Fidalgo), sai.gu@surrey.ac.uk (S. Gu).

http://dx.doi.org/10.1016/j.fuproc.2016.10.012

Nomenclature

k_0	pre-exponential factor, s^{-1}
E_a	activation energy, J/mol
c_p	specific heat capacity, J/kg K
E	electric field, V/m
H	magnetic field, A/m
S	yield of remaining solid
L	yield of condensable gas
G	yield of non-condensable gas
k_{0w}	wave number of free space
T	temperature, K
Po	input power, W
Q	heat source, W/m^3
Q_b	boundary heat Source, W/m^2
N_i	mass flux of species, kg/m^2s
u	velocity along x direction, m/s
v	velocity along y direction, m/s
w	velocity along z direction, m/s
h	heat transfer coefficient, $W/(m^2\ K)$
Δh_L^0	heat of reaction of lignin to condensable gas, J/kg
Δh_G^0	heat of reaction of lignin to non-condensable gas, J/kg
p	pressure, Pa
t	time, s
f	frequency, 1/s
d	pore diameter, m
n	unit normal
k	thermal conductivity of methane, W/m K
k_{eff}	effective thermal conductivity, W/m K
R	universal gas constant
M_i	mean molecular weight of the species, kg/kmol
x, y, z	coordinate along cavity width, depth and height
ϕ	porosity, dimensionless
ρ	density, kg/m^3
ϕ	porosity, dimensionless
σ	electrical conductivity, S/m
μ	gas phase viscosity, Pa · s
ϵ_r	relative permittivity, dimensionless
μ_r	relative permeability, dimensionless
ϵ_0	permittivity of free space, $A^2\ s^4/(m^3\ kg)$
μ_0	magnetic permeability of free space, N/A^2
κ	permeability, m^2
ω	angular frequency, rad/s
σ_{sb}	Stefan Boltzmann Constant
ω_e	emissivity, dimensionless

Subscripts

S	remaining solid
L	condensable gas
G	non-condensable gas
N_2	nitrogen
0	initial
g	gas phase
eff	effective value

properties of the materials. One of the main issues on the application of microwaves to biomass processing is that most of the common biomass feedstocks are poor microwave absorbers and they generally need to be mixed with effective microwave absorbers. Materials such as activated carbon and other carbon materials, metal oxide or silicon carbide are typically used as microwave absorbers in the microwave-assisted pyrolysis of biomass [5,8,9].

Microwave assisted pyrolysis of different biomass has been largely investigated, including, pulp mill sludge [10], saw dust [11,12], agricultural wastes [13], wheat straw bales [14], lignin [15,16], coffee hull [17], rice straw [18], sewage sludge [8], Douglas fir [19], micro-algae [20], oil palm biomass [21] and coal [22] . While there have been several experimental studies on microwave assisted heating of biomass [23,24], comparatively only few theoretical studies have been published [25–27]. The interaction among the number of physics involved in the process, including electromagnetic field, heat and mass transfer, fluid flow and reaction kinetics, along with the heterogeneous and temperature-dependent properties of the biomass, make the microwave assisted pyrolysis a complex process to investigate. However, numerical studies on microwave-assisted pyrolysis can provide new knowledge about the fundamentals of the process which are still unknown to a large degree, and aid upscaling the technology by better understanding the relationship between optimum operating conditions and product streams.

The available modelling studies describe the microwave assisted pyrolysis of wood using 2D mathematical models [25–27]. Despite they are helpful in capturing the qualitative features of the process, they do not provide much information on the temperature and concentration profiles within the biomass sample. In addition, the kinetic model parameters used in all the previous studies were derived from experiments with conventional heating as heat source [25–27]. The aim of this paper is to provide a better understanding of the interactions between the chemical and physical mechanisms governing the microwave-assisted pyrolysis process. This study builds upon previous work and develops a comprehensive 3D model of the process in order to address the change in temperature and simultaneous formation of products within the biomass bed. A lumped kinetic model derived from the microwave pyrolysis of kraft lignin by Farag et al. [15] is used in this work. To the best of our knowledge, this is the first time a 3D coupled mathematical model has been developed to predict and visualize dynamically the multiphysical behaviour of the whole integrated microwave pyrolysis system, including electromagnetic field, fluid flow, heat transfer, mass transfer and chemical reactions.

2. Model formulation

2.1. Material properties

Accurate reaction kinetic models are very important to determine the product distributions in a numerical analysis of pyrolysis. However very few detailed kinetic studies are available on biomass pyrolysis assisted by microwave heating. One recent study by Farag et al. [15] describes the microwave pyrolysis of kraft lignin and includes a kinetic model describing the formation of three lumped pyrolysis products: non-condensable volatiles (or gas fraction), condensable volatiles (or liquid fraction) and remaining solid. In this work, 'kraft lignin' is considered as a model biomass feedstock and the kinetic model proposed by Farag et al. [15] is used for the numerical analysis. Since lignin is one of the major constituent of woody biomass (20 –30 wt.%), the dielectric and thermal properties of wood were assumed as the best available approximation to the lignin properties which are not readily available in literature [32]. In accordance with the experiments performed by Farag et al. [15], the numerical analysis considered an initial mixture of lignin and char (30 wt.%) as a feedstock. Char was added to improve the absorption of microwaves. The relative permittivity of the mixture of lignin and char was determined from the data of various wood-char mixtures provided elsewhere [33]. Table 1 summarizes the values of the feedstock properties input to the model.

Table 1
Input parameters (material property values) used in the model.

ρ_{S_0}	700 kg/m^3	[28]
k_g	0.026 W/mK	[29]
ϕ_0	0.4	[30]
$k_{s_{x0}}$	0.098 W/mK	[30]
$k_{s_{y0}}$	0.098 W/mK	Estimated
$k_{s_{z0}}$	0.259 W/mK	[30]
ω_e	0.6	[27]
μ	3×10^{-5} Pa • s	[27]
d	4×10^{-5} m	[27]
κ_x	2.2×10^{-16} m^2	[30]
κ_y	2.2×10^{-16} m^2	Estimated
κ_z	9.7×10^{-14} m^2	[30]
M_{N_2}	28 kg/kmol	[27]
M_G	30 kg/kmol	[27]
M_L	95 kg/kmol	[27]
Δh_L^0	420 kJ/kg	[31]
Δh_G^0	420 kJ/kg	[31]
h	10 W/(m^2 K)	Estimated

2.2. Geometry

A schematic of the geometry used in the model is shown in Fig. 1. Although the kinetic model proposed by Farag et al. [15] has been used, the numerical model has been developed for a generic multimode microwave oven (cavity dimensions 33 × 23 × 29.5 cm) operating at a frequency of 2.45 GHz rather than the microwave system used by Farag et al. [15]. Microwave radiation is directed from the magnetron to the cavity through a rectangular waveguide (5 × 1.8 × 7.8 cm) operating in the TE_{10} mode. The walls of the oven and the waveguide were assumed to be made of copper. Biomass bed was assumed to be cylindrical (3 cm × 3 cm) and placed at the center of the microwave cavity. A vertical symmetry cut through the oven, waveguide and biomass bed was applied in order to reduce computational expense of the model.

2.3. Governing equations

The mathematical model describing the dynamics of lignin pyrolysis is based on the earlier work on pyrolysis of wood [25-27,30,34]. The model uses the porous solid approach (Eulerian description) to consider the solid biomass [35].

Various assumptions were considered in the model: (a) local thermodynamic equilibrium suggesting that all the phases are at the same temperature; (b) ideal gas flow; (c) no change in total volume; and, (d) negligible shrinkage, crack formation, presence of moisture and mass transfer by diffusion.

The reaction rate expressions for the formation of the liquid fraction, gas fraction and remaining solid are as given by Eqs. (1), (2) and (3) respectively [15].

$$r_L = k_{0_L} e^{(-E_{a_L}/RT)}(S - S_\infty) \tag{1}$$

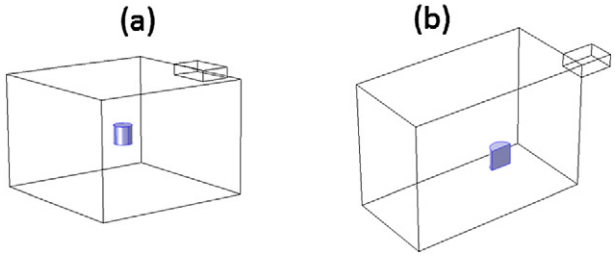

Fig. 1. Schematic of the (a) full microwave cavity with the biomass sample and (b) symmetrical geometry used in the model

$$r_G = k_{0_G} e^{(-E_{a_G}/RT)}(S - S_\infty) \tag{2}$$

$$r_S = -k_{0_S} e^{(-E_{a_S}/RT)}(S - S_\infty) \tag{3}$$

where, k_0 is the pre-exponential factor, E_a is the apparent activation energy, T is the reaction temperature, R is the universal gas constant and S is the solid yield at time t of the reaction. Subscripts S, L, G refer to remaining solid, liquid and gas respectively. S_∞ is the final solid yield, obtained from the experimental data provided in [15]. The kinetic model parameters used in the model are summarized in Table 2.

The 3D unsteady formulation of the governing equations describing the process is based on the mass conservation for the solid, condensable volatiles and non-condensable gas.

$$\frac{\partial \rho_S}{\partial t} = -(r_L + r_G) * \rho_{S_0} \tag{4}$$

$$\frac{\partial \phi \rho_L}{\partial t} + \frac{\partial \rho_L u}{\partial x} + \frac{\partial \rho_L v}{\partial y} + \frac{\partial \rho_L w}{\partial z} = r_L * \rho_{S_0} \tag{5}$$

$$\frac{\partial \phi \rho_G}{\partial t} + \frac{\partial \rho_G u}{\partial x} + \frac{\partial \rho_G v}{\partial y} + \frac{\partial \rho_G w}{\partial z} = r_G * \rho_{S_0} \tag{6}$$

where, ρ_S, ρ_L, ρ_G are the densities of remaining solid, liquid and the non-condensable gas respectively and ϕ is the porosity described by Eq. (7),

$$\phi = 1 - \rho_S/\rho_{S_0}(1 - \phi_0) \tag{7}$$

In addition, the total continuity equation, the state equation (considering the total gas-vapour phase density) and the inert nitrogen density are described by Eqs. (8), (9) and (10), respectively.

$$\frac{\partial \phi \rho_g}{\partial t} + \frac{\partial \rho_g u}{\partial x} + \frac{\partial \rho_g v}{\partial y} + \frac{\partial \rho_g w}{\partial z} = r_L + r_G \tag{8}$$

$$\rho_g = \frac{pM_g}{RT} \tag{9}$$

$$\rho_{N_2} = \rho_g - (\rho_L + \rho_G) \tag{10}$$

where M_g is the mean molecular weight of the gas/vapour phase mixture $= (M_{N_2}\rho_{N_2} + M_G\rho_G + M_L\rho_L)/\rho_g$, kg/kmol, p is the pressure and ρ_g is the density of the gas/vapour phase mixture.

The energy conservation is obtained by assuming thermal equilibrium between solid and gas phases and is given by Eq. (11),

$$(\rho c)_{\text{eff}} \frac{\partial T}{\partial t} + \rho_g c_g u \cdot \nabla T = \nabla \cdot (k_{\text{eff}} \nabla T) - (r_L \Delta h_L^0 + r_G \Delta h_G^0)\rho_{S_0} + Q \tag{11}$$

$$(\rho c)_{\text{eff}} = (1 - \phi)\rho_S c_S + \phi \rho_g c_g \tag{12}$$

$$\rho_g c_g = \rho_L c_L + \rho_G c_G + \rho_{N_2} c_{N_2} \tag{13}$$

$$c_S = 1500 + T[\text{J}/(\text{Kg} \cdot \text{K})] \tag{14}$$

Table 2
Kinetic model parameters used in the model for microwave pyrolysis of lignin (values from [15]).

k_{0_L}	22 min^{-1}
k_{0_G}	6 min^{-1}
k_{0_S}	7 min^{-1}
E_{0_L}	29 kJ/mol
E_{0_G}	22 kJ/mol
E_{0_S}	19 kJ/mol

$$c_L = -100 + 4.4T - 1.57e^{-3}T^2[\mathrm{J/(Kg\cdot K)}] \quad (15)$$

$$c_G = 700 + 0.629T - 1.91e^{-4}T^2[\mathrm{J/(Kg\cdot K)}] \quad (16)$$

$$c_{N_2} = 972 + 0.15T[\mathrm{J/(Kg\cdot K)}] \quad (17)$$

Here, c refers to the specific heat capacity, Δh_L^0 and Δh_G^0 is the heat of reaction of lignin conversion to condensable and non-condensable gases respectively and Q is the heat source. The expressions for the specific heat are taken from [27]. Heat transfer to and from the biomass sample occurs through conduction, convection and radiation. Thus the effective thermal conductivity k_{eff} is given as:

$$k_{\mathrm{eff}_x} = (1-\phi)k_{S_x} + \phi k_g + k_{rad}, \quad (18)$$

$$k_{\mathrm{eff}_y} = (1-\phi)k_{S_y} + \phi k_g + k_{rad}, \quad (19)$$

$$k_{\mathrm{eff}_z} = (1-\phi)k_{S_z} + \phi k_g + k_{rad} \quad (20)$$

$$k_{S_x} = k_{S_{xo}}T/T_0, \quad (21)$$

$$k_{S_y} = k_{S_{yo}}T/T_0, \quad (22)$$

$$k_{S_z} = k_{S_{zo}}T/T_0, \quad (23)$$

$$k_{\mathrm{rad}} = 4\frac{\phi}{1-\phi}\omega\sigma_B dT^3 \quad (24)$$

The superficial velocity of the condensable and non-condensable gas mixture is described by the Darcy Law:

$$u = -\frac{\kappa_x}{\mu}\frac{\partial p}{\partial x}, v = -\frac{\kappa_y}{\mu}\frac{\partial p}{\partial y}, w = -\frac{\kappa_y}{\mu}\left(\frac{\partial p}{\partial z} + \rho_g g\right) \quad (25)$$

where, κ is the permeability, μ is the gas phase viscosity and u, v and w refer to the velocity along x, y and z direction respectively.

The electric field distribution is obtained by solving for the electric field vector E inside the waveguide and the microwave cavity.

$$\nabla \times \left(\mu_r^{-1}\nabla \times E\right) - k_{0w}^2\left(\epsilon_r - \frac{j\sigma}{\omega\epsilon_0}\right)E = 0 \quad (26)$$

where, E, electric field intensity (V/m); $\epsilon_r = \epsilon' - i\epsilon''$, complex relative permittivity; $\omega = 2\pi f$, angular wave frequency (rad/s); f, frequency (Hz), μ_r, relative permeability, σ, electrical conductivity (S/m), ϵ_0, permeability of free space. The wavenumber of free space, k_{0w} is defined as $k_{0w} = \omega/c_0$. c_0 is the speed of light in vacuum.

The heat source term, Q in the energy balance equation is calculated from the volumetric power generated by dielectric heat dissipation in the biomass sample due to microwave exposure and is expressed as:

$$Q = 2\pi f\epsilon_0\epsilon''|E|^2 \quad (27)$$

The coupled governing equations described above were solved using Finite Element Method in COMSOL Multiphysics v 5.0. The governing equations describing the electromagnetics were solved at the fixed frequency value of 2.45 GHz, and the FGMRES Iterative Solver which uses the restarted flexible generalized minimum residual method was used. The porous media fluid flow, heat and mass transfer equations were solved using the segregated solver in COMSOL.

2.4. Boundary conditions

The governing equations are solved based on the boundary conditions described below:

2.4.1. Electric field equation

Walls of the microwave cavity and the waveguide are considered to be made of copper in this model and thus the electric field will only penetrate short distance outside the boundary. This penetration is accounted using a useful approximation known as the impedance boundary condition (IBD), which avoids the need to include another domain in the model while ensuring even the small losses are accounted. IBD is defined as,

$$\sqrt{\frac{\mu_0\mu_r}{\epsilon_0\epsilon_r - j\sigma/\omega}}n \times H + E - (n\cdot E)n = 0 \quad (28)$$

where n is the unit normal, H is the magnetic field. The fact that the electric current cannot flow and the tangential magnetic field vanishes at the symmetrical boundary is represented as following,

$$n \times H = 0 \quad (29)$$

The applied input power value at the entrance of the rectangular waveguide is specified as,

$$P = P_0 \quad (30)$$

2.4.2. Energy balance equation

The condition described by Eq. (31) is specified on the surface of the biomass to account for the heat source on the boundary due to the electromagnetic loss.

$$Q_b = n\cdot(k\nabla T) \quad (31)$$

The outer surface of the biomass also loses heat due to convection and radiation. These losses are represented by Eq. (32),

$$n\cdot(k\nabla T) = h(T_0 - T) + \omega_e\sigma_{sb}(T_0^4 - T^4) \quad (32)$$

where, Q_b is the boundary heat source, h is the heat transfer coefficient and ω_e is the emissivity of the biomass sample. For simplicity, a common heat transfer coefficient h is considered on all the outer boundaries of the biomass sample.

The temperature gradient across the symmetrical boundary is zero, which is implemented by the following boundary condition

$$n\cdot(k\nabla T) = 0 \quad (33)$$

2.4.3. Darcy Law

At the upper and lateral surfaces of the biomass sample, the pressure is specified as atmospheric pressure

$$p = p_{atm} \quad (34)$$

At the bottom surface and the symmetrical boundary, a no flow boundary condition is specified as,

$$n\cdot(k\nabla p) = 0 \quad (35)$$

At the symmetrical boundary, vanishing shear stresses and no penetration condition is implemented as following

$$u \cdot n = 0 \quad \text{and} \quad K - (K \cdot n)n = 0$$
$$\text{where} \quad K = \mu \left(\nabla u + \nabla u^T \right) n \tag{36}$$

2.4.4. Mass conservation

At the bottom surface of the biomass sample, there is negligible density of the liquid and gas products, represented as following,

$$\rho_L = \rho_G = 0 \tag{37}$$

At the symmetrical boundary, there is no mass flux in the normal direction across the boundary,

$$-n \cdot N_i = 0 \tag{38}$$

3. Results and discussion

3.1. Electric field and temperature profiles

Fig. 2 shows the normal electric field distribution in the microwave cavity with and without the biomass sample for applied input power of 1200 W. As can be seen clearly from Fig. 2, areas of low and high microwave energy are found in the multimode microwave cavity. Introduction of the biomass sample changes the electric field distribution inside the cavity and the normal electric field drops from an earlier maximum of about 4×10^4 V/m to 3.5×10^4 V/m. Absorption of microwave energy by the sample and the reflections from the walls of the microwave cavity redistribute the electromagnetic field. This result relates to the importance of the position of any sample inside the cavity, as not all regions are exposed to equal field intensity.

Once the mixture of lignin and char is exposed to the electromagnetic waves, it rapidly heats up due to the continuous re-alignment of charged particles which are restrained to move in a delimited region leading to friction. The energy conversion can be visualized by means of the electromagnetic power loss density shown in Fig. 3. As can be seen the electromagnetic power loss density is nearly zero in the entire microwave cavity except throughout the biomass sample (Fig. 3A), because of its ability to absorb the microwave radiation. The electromagnetic power loss density reaches a maximum of about 5×10^6 W/m^3 at the center of the biomass bed (Fig. 3B). Geometry of the microwave cavity, geometry and size of the biomass (lignin) sample and its dielectric and thermal properties determine how the sample is heated on exposure to microwave radiation. The rate and intensity of the electromagnetic power loss density are largely dependent on the complex relative permittivity and the dielectric loss tangent of the sample. Higher heat loss represents a higher conversion of electromagnetic to thermal energy.

In addition, both the electric field distribution and the power loss density in the microwave cavity are dependent on the applied input power. In order to evaluate the relation between input power and electric field distribution and their combined effect on the temperature distribution in the biomass sample, two different applied input power values were studied, Po = 800 W and Po = 1200 W after 10 min. A time of 10 min was selected because a fairly steady temperature is reached after this time. Fig. 4 shows the normal electric field intensity and the corresponding temperature distribution within the biomass bed for the two applied input powers.

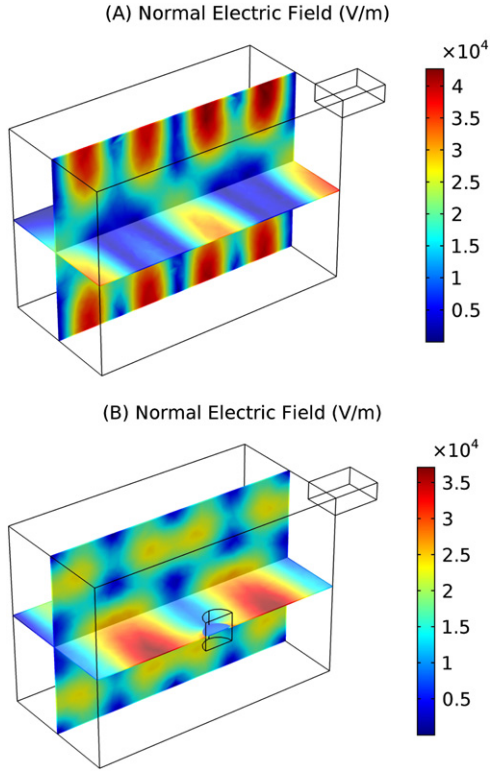

Fig. 2. Normal electric field distribution (V/m) in the microwave cavity without the biomass sample (A) and with the biomass sample (B), at applied input power Po = 1200 W.

Higher input power results in a higher electric field intensity (comparing A with B in Fig. 4) which in turn gives rise to faster temperature increase in the biomass sample considering the same time interval (comparing C with D in Fig. 4). As expected the temperature distribution in the biomass sample reproduces the qualitative shape of the electric field distribution. The important feature of the microwave heating, i.e. the volumetric heating effect, with the maximum temperature at the center and decreasing outward, can also be clearly observed from the simulation results.

The volumetric heating effect is illustrated more clearly in Fig. 5, which shows the volume and slice colour plots of temperature profiles in the biomass sample with increasing time, for applied power, Po = 1200 W.

As can be seen, the center of the biomass bed sample is hottest at any given time and the temperature is lower towards the external surface. The overall temperature in the sample increases with time while also enlarging the heating zone. This behaviour is consistent with previous experimental and simulation results [27,36].

The formation of hot spots within the biomass bed significantly depends on the position of the sample in the microwave cavity, the heat loss from the walls of the sample due to convection and radiation and the heterogeneity of dielectric properties throughout the sample due to differences between the lignin and char. In addition, dielectric properties of the biomass sample change with the increase in temperature, as the lignin decomposes into char and volatiles. The present model assumes that the biomass sample is placed exactly at the center of the cavity and a single heat transfer coefficient ($h = 10$) has been used for all the outer walls of the sample. Moreover, due to lack of the availability of accurate space and temperature functions, the change in dielectric properties has not been included in the current simulation. All these assumptions explain the exactly concentric temperature increase with a single hot spot at the center of the biomass sample.

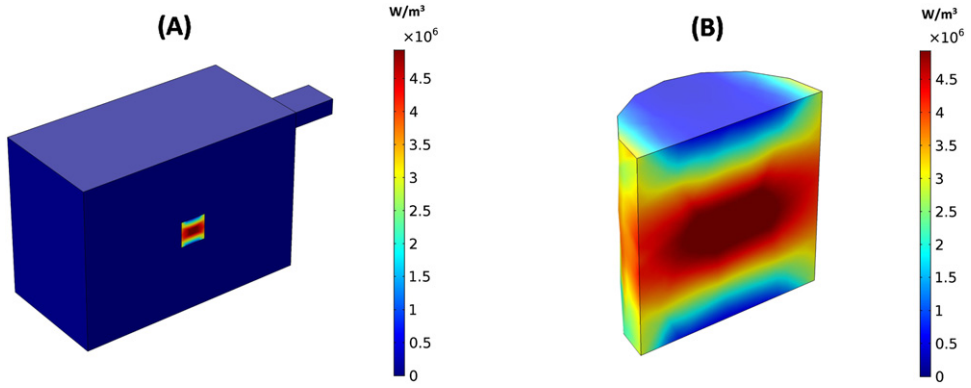

Fig. 3. Electromagnetic power loss density (W/m^3) at applied input power Po = 1200 W in the entire microwave cavity with the biomass sample (A) and zoomed view of electromagnetic power loss density in the biomass sample alone (B).

3.2. Conversion profiles

The kinetic mechanism used in the present study is based on the parameters derived using the experimental data of gas and liquid fraction yields as a function of temperature [15]. Before presenting the product yield concentration profiles in the biomass bed, the implementation of the reaction kinetics in the 3D model is validated by comparing the predicted liquid and gas product yields with those derived from the experimental data [15], as shown in Fig. 6. The predicted liquid and gas fraction yields represented here, are derived from the average concentration values of the different products over the exterior surface of the lignin sample (except the bottom boundary, which is impermeable).

A close agreement between experimental data points and simulation predictions of the product yields as a function of temperature, suggests that the kinetic model has been correctly implemented and coupled with the transport and the electromagnetic governing equations. This coupled 3D numerical model can thus be reliably used for studying the microwave-assisted pyrolysis of kraft lignin.

It should be noted however, that the variation of product yield concentrations as a function of time are not reported [15] and these profiles depend on the specific design and setup of the microwave system being used for the study. Thus comparison of transient variations of product yield concentrations are beyond the scope of this study. The goal of this work is not to optimize the generic microwave reactor for pyrolysis of kraft lignin but to develop and demonstrate the capabilities of 3D mathematical model that include all the important physics of the process. 3D model allows us to visualize electric field, temperate and concentration profiles in all space dimensions and develop better understanding of chemical and physical phenomena occurring during this process. It is understood that more detailed investigations, with experiments designed for

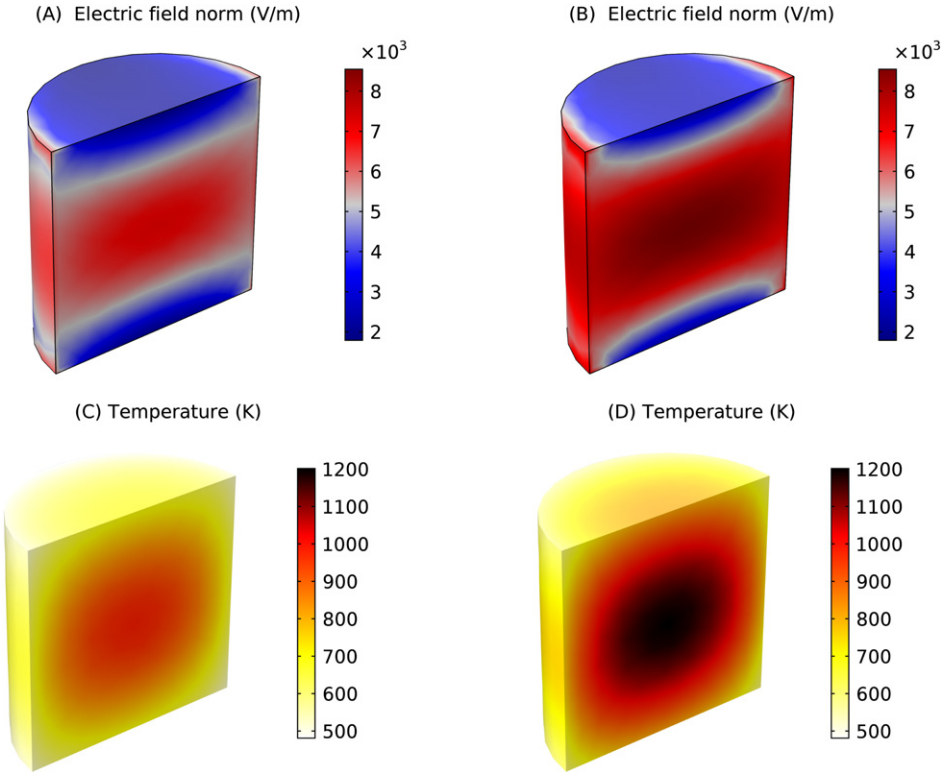

Fig. 4. Predicted normal electric field distribution in the biomass sample (A and B) and temperature distribution (C and D) for applied input power of Po = 800 W and Po = 1200 W respectively.

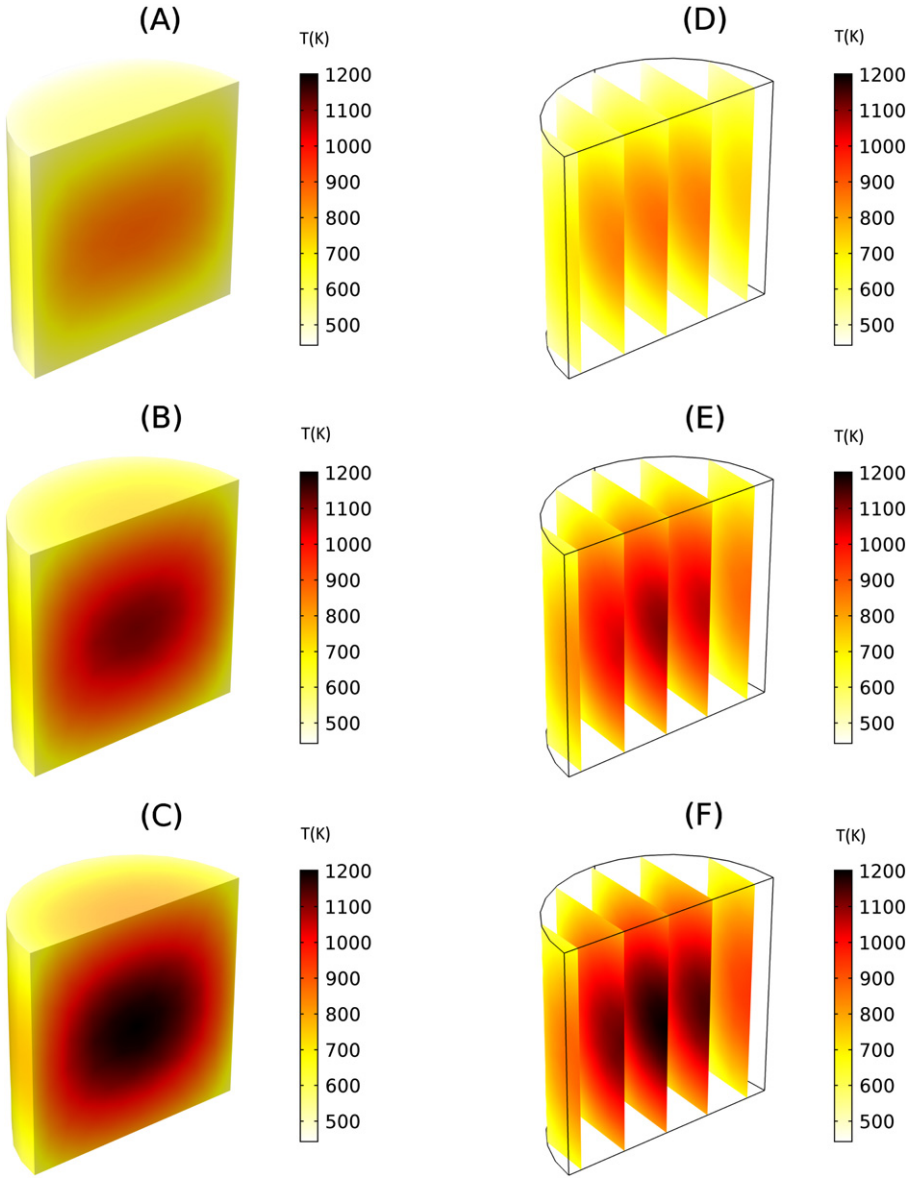

Fig. 5. Volume plots (A, B and C) of temperature distribution in the biomass sample after (a) 200s, (b) 400s and (c) 600s and the corresponding slice plots (D, E and F) for applied input power, Po = 1200 W.

a specific microwave system and biomass need to be carried out for extensive comparison with experiments. A more comprehensive study, including modelling as well as experiments is planned for the near future.

Figs. 7 and 8 show the 3D colour plots for predicted percentage yields of liquid fraction (condensable gas) and gas fraction (non-condensable gas) respectively, after 150, 300, 450 and 600 s of microwave exposure at input power Po = 1200 W. As can be seen from Figs. 7 and 8, the distribution of condensable and non-condensable gases in the biomass bed qualitatively reproduces the same shape as the distribution of temperature. Maximum yield is at the center of the sample and increases concentrically towards the walls of the bed as the temperature in outer region increases. The exterior surface of lignin which is comparatively cooler than the center of the sample, is the last to get decomposed. Both condensable and non-condensable gases slowly escapes out from the lateral and top surfaces of the sample and eventually (further to 600 sec, which is not shown here) the average concentration of both the fractions begins to decrease. In accordance with the conversion values predicted in Fig. 6, the maximum percentage yield conversions of condensable and non-condensable gases are about 35 and 28% respectively.

As lignin decomposes into char and volatiles, the permeability of the remaining solid increases (as permeability of char is higher than that of lignin). In this model however char and lignin are indistinguishable and change in permeability cannot be specified. For this reason, the model would predict a much slower release of the volatiles compared with the actual experiments. This reinforces the importance of using accurate kinetics and material properties.

It should be noted that microwave assisted pyrolysis of biomass is a complex process, depending on a multitude of process parameters including materials properties and operating conditions. The use of a simple lumped kinetic model and certain assumptions in the material properties, limits the applicability of the results obtained from this analysis. However, based on the detailed representation of the electric field, temperature and concentration profiles in the biomass bed volume, the model helps to overcome the limitations to obtain a realistic visualization of the decomposition process through

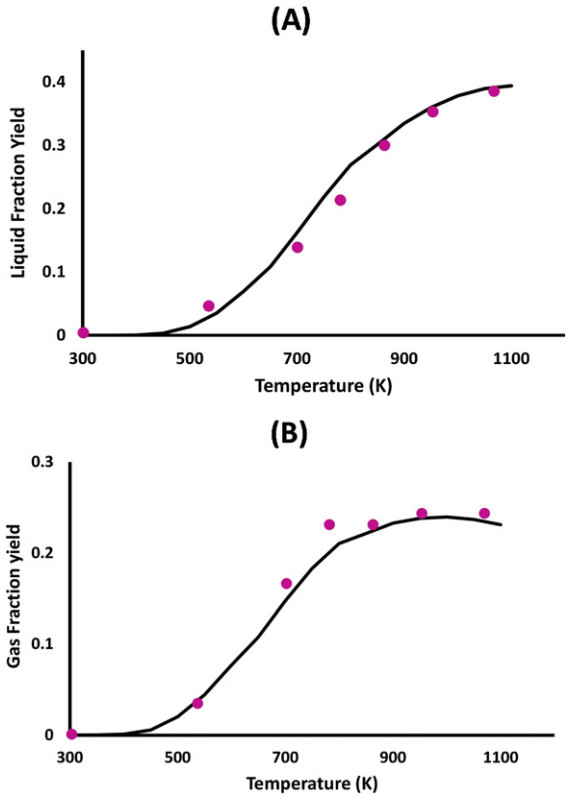

Fig. 6. Comparison of predicted (solid lines) and experimental (pink circles) yields of (A) liquid and (B) gas fractions as a function of temperature.

experiments or 2D approaches. It allows one to study the rate of variation of important process variables in all three directions. This becomes more important for biomass, as they are non-homogeneous and have a natural anisotropy, leading to a variation in physical properties in different directions.

The effect of different process parameters such as the type, size and shape of biomass sample, type (multimode or unimode) and dimensions of the microwave cavity, position of the biomass sample inside the microwave cavity and frequency and microwave power, can be individually investigated in great detail. This is seldom possible through experiments. Detailed 3D models are expected to be valuable for analysing, designing, optimizing and facilitating the scale-up of the system. A more extensive study of how biomass conversion and selectivity for a specific product are influenced by the operating conditions, and an insight of how these factors affect the energy cost and efficiency of the system, is planned for the near future.

3.3. Effect of sample size and position

As an example of the applicability of the model, the influence of the biomass sample size and position within the cavity, on the temperature profile has been evaluated. As can be seen from Fig. 9, increasing sample size by 1.5 times the original, results in a slower heating process and changes the heating profile. Fig. 9B shows that for a larger size sample the temperature distribution is no longer concentric but more lateral from the centerline. The temperature profile largely depends on the electric field distribution and the dielectric properties of the biomass sample. When the sample size is increased 1.5 times, the electric field distribution in the sample changes. Referring back to Fig. 4A, it can be seen that the maximum for electric field is at the center for the smaller sample size. The electric field maxima for the larger sample moves closer to the side walls (not included here). This change in distribution creates two maxima for electric field in the larger sample, which results in the temperature distribution to become more lateral and not concentric.

The heating profile determines the direction and the flow rate of the volatiles from the sample and it is thus a crucial deterministic factor when designing the system for microwave pyrolysis of biomass. Moreover, a considerable variation of electric field over the dimensions of the sample can lead to non-uniform heating and consequently it is very important to optimize the sample bed dimensions.

Fig. 10 highlights the influence of the position of the sample within the microwave cavity on the heating rate and temperature profile. This figure was generated by overlapping the predictions from three individual simulation runs with samples placed at three different locations, near to right wall, center and near to the left wall of the microwave cavity.

All the three samples show different temperature profiles varying from a minimum temperature of 400 K to a maximum of 1450 K. The amount of power absorbed and converted to heat strongly depends on the electric field. As described earlier in Fig. 2, the electric field distribution in the microwave cavity is not uniform and alters further once a sample is placed inside. Therefore, despite the similar dielectric properties of the three samples, the amount of power absorbed by each of them is different because of the differences in the electric field distribution. The sample on the left absorbs maximum power and is significantly hotter than the other two samples in the same time span.

The maximum temperature achieved in the center and the right side samples are similar, however the temperature distribution is not the same. Also while the samples on the left and the center are heated symmetrically with the hottest region at the center, the one on the right does not show symmetric heating. These differences in the heating rate and heating profiles caused by changes in the placement of the sample, can lead to substantial differences in product distributions and flow rates.

Similar to the two examples that have been illustrated here, the 3D model of the microwave assisted pyrolysis can be used to investigate other important parameters that influence the process. Provided that appropriate reaction kinetics are available and the model is properly validated, it can be used to study various types of biomass in different microwave reactors to determine the optimum conditions for maximizing the yields of required products and energy efficiency of the system.

Further improvements can be implemented to the model by accounting for important factors which were not included in the present study due to the lack of available data, such as the thermal and dielectric properties of the biomass as a function of temperature, accurate heat transfer coefficients, moisture evaporation, or inclusion of secondary reaction to the kinetic model. The incorporation of these additional factors will result in a more credible tool to optimize the microwave pyrolysis process working in conjunction with experiments. Extending the capabilities of the current model by addressing some of the above shortcomings, along with detailed experiments for specific microwave system and biomass are planned for the near future.

4. Conclusion

In this work, a numerical study of the microwave assisted pyrolysis of lignin was carried out by developing a comprehensive three-dimensional mathematical model including all the important physics that affect the process. A lumped kinetic model considering three parallel reactions converting kraft lignin into liquids, non-condensable gas and remaining solids was used to obtain the

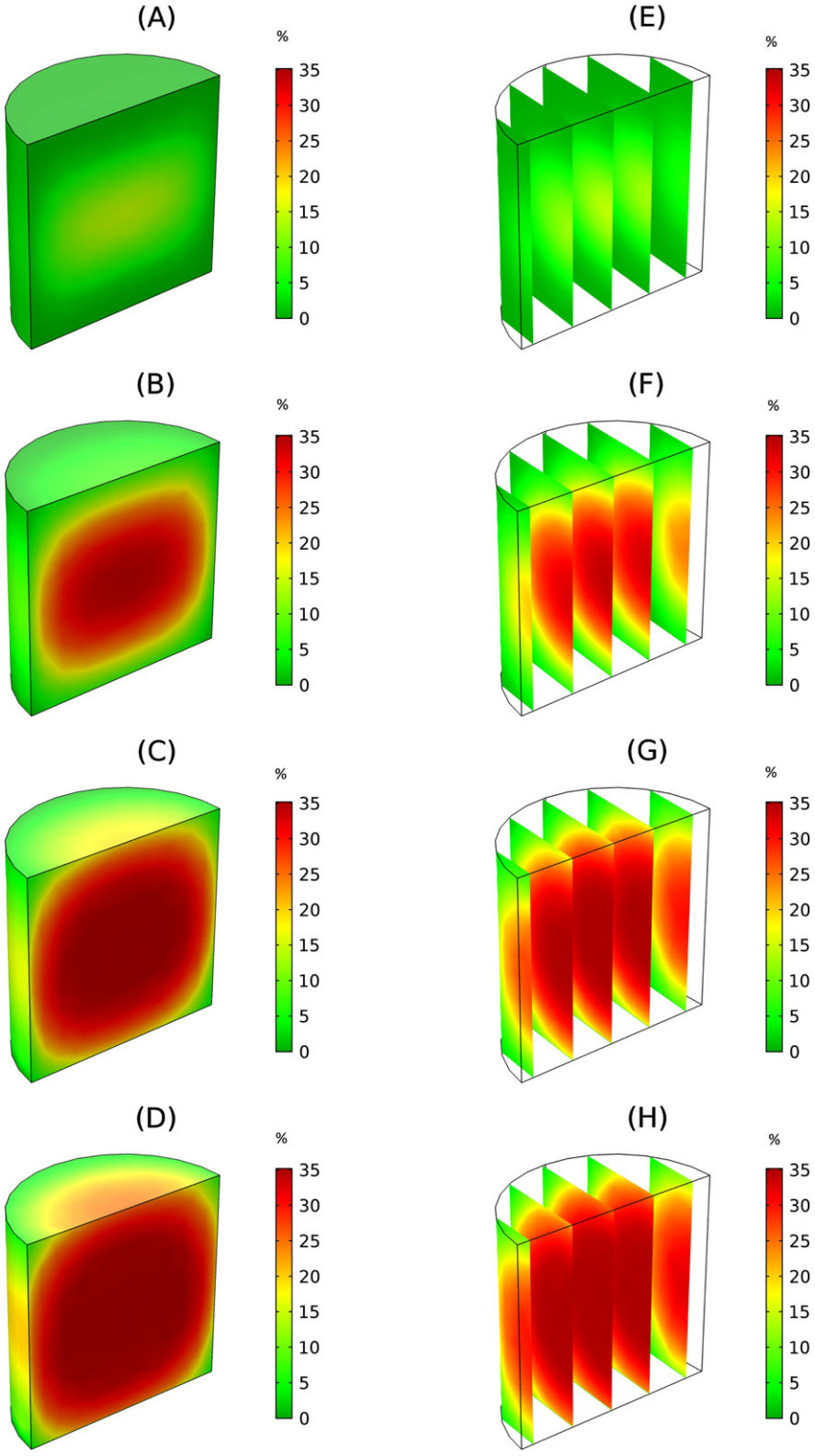

Fig. 7. Volume plots of percentage (%) yield of the liquid fraction in the biomass sample after (A) 150s, (B) 300s, (C) 450s and (D) 600s and the corresponding slice plots (E–H) for applied power, Po = 1200 W.

pyrolysis product distributions, and validated against experimental results. The comparison of the electric field distribution within the microwave cavity showed that the introduction of the biomass sample changes the electric field profile and its maximum value. 3D slice plots of the temperature distribution within the biomass samples obtained from the model allowed visualizing the volumetric heating effect of microwaves, showing concentric temperature profiles whose values decreased from the center towards the external surface

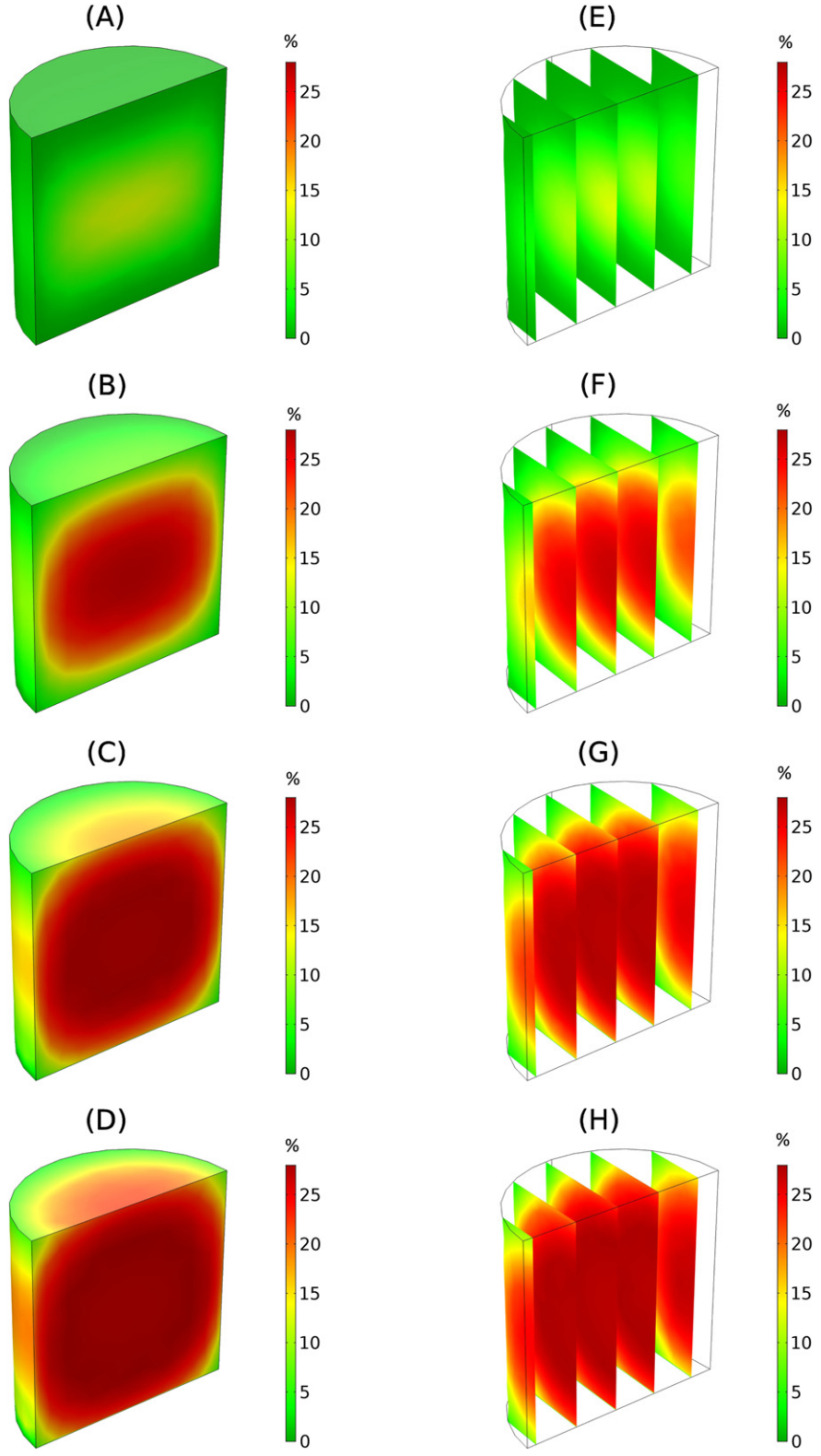

Fig. 8. Volume plots of percentage (%) yield of the gas fraction in the biomass sample after (A) 150s, (B) 300s, (C) 450s and (D) 600s and the corresponding slice plots (E–H) for applied power, Po = 1200 W.

of the sample bed. Liquid product yield profiles were presented illustrating a concentric increase with time and the exit of the products from the lateral and top surfaces. Moreover, the applicability of the 3D model for the study of different parameters affecting the microwave pyrolysis of biomass was confirmed by studying the influence of the biomass (lignin) sample size and position in the microwave cavity on the temperature distribution.

The model developed in this work was demonstrated to be useful for investigation of different process parameters of the microwave pyrolysis of kraft lignin on a generic microwave oven. The model

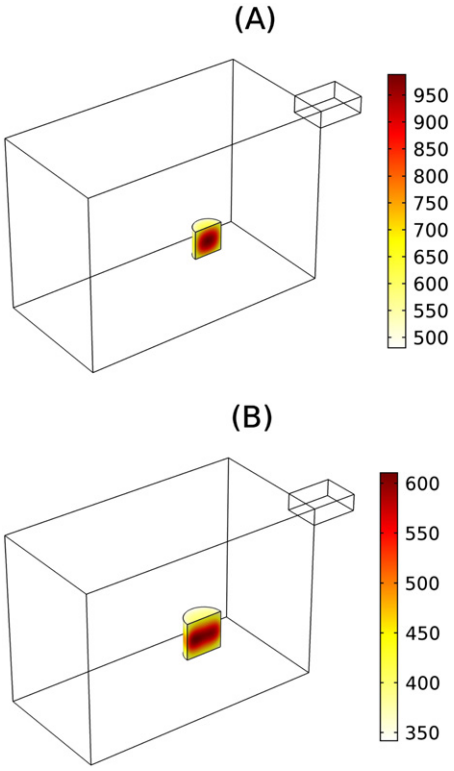

Fig. 9. Temperature distribution (K) in the biomass bed for two different sample sizes at applied input power of Po = 800 W after 600s.

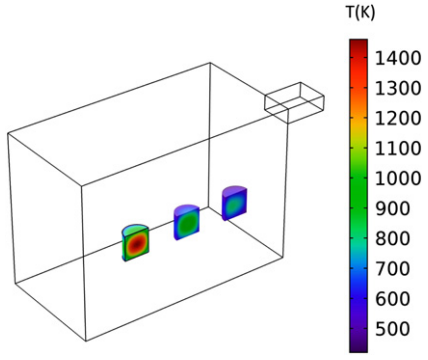

Fig. 10. Temperature distribution (K) in the three biomass samples placed after 600s at different locations along the centerline of the microwave cavity for input power of Po = 800 W.

however, must be customized for each specific biomass and type of microwave system being used. It can be further improved by including more accurate material properties (which are specific to the biomass being studied and vary as a function of changing process conditions) and more complex/detailed reaction kinetics, which include secondary reactions and individual rate constants for a variety of products that are formed during the pyrolysis process, as compared to the lumped kinetic model used in this work.

Acknowledgments

The authors would like to gratefully acknowledge the European Commission and the Engineering and Physical Sciences Research Council (EPSRC) UK for the financial support of this work through the FP7 Marie Curie IRSES iComFluid project (reference: 312261) and EPSRC grants EP/K036548/2 and EP/M013162/1.

References

[1] M. Jahirul, M. Rasul, A. Chowdhury, N. Ashwath, Biofuels production through biomass pyrolysis - a technological review, Energies 5 (12) (2012) 4952–5001.
[2] A. Bridgwater, Review of fast pyrolysis of biomass and product upgrading, Biomass Bioenergy 38 (2012) 68–94.
[3] S. Lam, H. Chase, A review on waste to energy processes using microwave pyrolysis, Energies 5 (10) (2012) 4209–4232.
[4] A. Zlotorzynski, The application of microwave radiation to analytical and environmental chemistry, Crit. Rev. Anal. Chem. 25 (1) (1995) 43–76.
[5] J. Menendez, A. Arenillas, B. Fidalgo, Y. Fernndez, L. Zubizarreta, E. Calvo, J. Bermdez, Microwave heating processes involving carbon materials, Fuel Process. Technol. 91 (1) (2010) 1–8.
[6] M. Gawande, S. Shelke, R. Zboril, R. Varma, Microwave-assisted chemistry: synthetic applications for rapid assembly of nanomaterials and organics, Acc. Chem. Res. 47 (4) (2014) 1338–1348.
[7] H. Will, P. Scholz, B. Ondruschka, Heterogeneous gas-phase catalysis under microwave irradiation - a new multi-mode microwave applicator, Top. Catal. 29 (3-4) (2004) 175–182.
[8] Y. Tian, W. Zuo, Z. Ren, D. Chen, Estimation of a novel method to produce bio-oil from sewage sludge by microwave pyrolysis with the consideration of efficiency and safety, Bioresour. Technol. 102 (2) (2011) 2053–2061.
[9] J. Menendez, M. Inguanzo, J. Pis, Microwave-induced pyrolysis of sewage sludge, Water Res. 36 (13) (2002) 3261–3264.
[10] A. Namazi, D. Allen, C. Jia, Microwave-assisted pyrolysis and activation of pulp mill sludge, Biomass Bioenergy 73 (2015) 217–224.
[11] H. Shang, R.-R. Lu, L. Shang, W.-H. Zhang, Effect of additives on the microwave-assisted pyrolysis of sawdust, Fuel Process. Technol. 131 (2015) 167–174.
[12] X.-H. Wang, H.-P. Chen, X.-J. Ding, H.-P. Yang, S.-H. Zhang, Y.-Q. Shen, Properties of gas and char from microwave pyrolysis of pine sawdust, BioResources 4 (3) (2009) 946–959.
[13] S.M.A. Aziz, R. Wahi, Z. Ngaini, S. Hamdan, Bio-oils from microwave pyrolysis of agricultural wastes, Fuel Process. Technol. 106 (2013) 744–750.
[14] X. Zhao, J. Zhang, Z. Song, H. Liu, L. Li, C. Ma, Microwave pyrolysis of straw bale and energy balance analysis, J. Anal. Appl. Pyrolysis 92 (1) (2011) 43–49.
[15] S. Farag, L. Kouisni, J. Chaouki, Lumped approach in kinetic modeling of microwave pyrolysis of kraft lignin, Energy Fuels 28 (2) (2014) 1406–1417.
[16] C. Peng, G. Zhang, J. Yue, G. Xu, Pyrolysis of lignin for phenols with alkaline additive, Fuel Process. Technol. 124 (2014) 212–221.
[17] A. Domnguez, J. Menndez, Y. Fernndez, J. Pis, J. Nabais, P. Carrott, M. Carrott, Conventional and microwave induced pyrolysis of coffee hulls for the production of a hydrogen rich fuel gas, J. Anal. Appl. Pyrolysis 79 (1-2 SPEC. ISS.) (2007) 128–135.
[18] Y.-F. Huang, P.-T. Chiueh, C.-H. Shih, S.-L. Lo, L. Sun, Y. Zhong, C. Qiu, Microwave pyrolysis of rice straw to produce biochar as an adsorbent for CO_2 capture, Energy 84 (2015) 75–82.
[19] Q. Bu, H. Lei, L. Wang, Y. Wei, L. Zhu, Y. Liu, J. Liang, J. Tang, Renewable phenols production by catalytic microwave pyrolysis of douglas fir sawdust pellets with activated carbon catalysts, Bioresour. Technol. 142 (2013) 546–552.
[20] Z. Hu, X. Ma, C. Chen, A study on experimental characteristic of microwave-assisted pyrolysis of microalgae, Bioresour. Technol. 107 (2012) 487–493.
[21] A. Salema, F. Ani, Microwave induced pyrolysis of oil palm biomass, Bioresour. Technol. 102 (3) (2011) 3388–3395.
[22] B.R. Reddy, R. Vinu, Microwave assisted pyrolysis of Indian and Indonesian coals and product characterization, Fuel Process. Technol. 154 (2016) 96–103.
[23] F. Mushtaq, R. Mat, F. Ani, A review on microwave assisted pyrolysis of coal and biomass for fuel production, Renew. Sustain. Energy Rev. 39 (2014) 555–574.
[24] W. Yunpu, D. Leilei, F. Liangliang, S. Shaoqi, L. Yuhuan, R. Roger, Review of microwave-assisted lignin conversion for renewable fuels and chemicals, J. Anal. Appl. Pyrolysis 119 (2016) 104–113.
[25] T. Ciacci, A. Galgano, C. Di Blasi, Numerical simulation of the electromagnetic field and the heat and mass transfer processes during microwave-induced pyrolysis of a wood block, Chem. Eng. Sci. 65 (14) (2010) 4117–4133.
[26] R. Tarchini, A. Galgano, C. di Blasi, Modeling the influences of pressure and velocity variations on the microwave-induced pyrolysis of wood, AIChE J. 58 (2) (2012) 610–624.
[27] R. Santaniello, A. Galgano, C. Di Blasi, Coupling transport phenomena and tar cracking in the modeling of microwave-induced pyrolysis of wood, Fuel 96 (2012) 355–373.
[28] L. Christopher, Integrated Forest Biorefineries, The Royal Society of Chemistry, London, 2012.
[29] C. Di Blasi, Heat, momentum and mass transport through a shrinking biomass particle exposed to thermal radiation, Chem. Eng. Sci. 51 (7) (1996) 1121–1132.
[30] M. Gronli, A Theoretical and Experimental Study of the Thermal Degradation of Biomass., (Ph.D. thesis). NTNU, Trondheim, Norway. 1996.
[31] W.-C. Chan, M. Kelbon, B. Krieger, Modelling and experimental verification of physical and chemical processes during pyrolysis of a large biomass particle, Fuel 64 (11) (1985) 1505–1513.

[32] T. Hatakeyama, H. Hatakeyama, Lignin, Thermal Properties of Green Polymers and Biocomposites Kluwer Academic Publishers, Dordrecht, 2004, pp. 171–215. (Ch. 5).
[33] S. Farag, A. Sobhy, C. Akyel, J. Doucet, J. Chaouki, Temperature profile prediction within selected materials heated by microwaves at 2.45 GHz, Appl. Therm. Eng. 36 (1) (2012) 360–369.
[34] M. Gronli, M. Melaaen, Mathematical model for wood pyrolysis-comparison of experimental measurements with model predictions, Energy Fuels 14 (4) (2000) 791–800.
[35] C. Di Blasi, Modeling chemical and physical processes of wood and biomass pyrolysis, Prog. Energy Combust. Sci. 34 (1) (2008) 47–90.
[36] M. Miura, H. Kaga, A. Sakurai, T. Kakuchi, K. Takahashi, Rapid pyrolysis of wood block by microwave heating, J. Anal. Appl. Pyrolysis 71 (1) (2004) 187–199.